Journal of Low Temperature Physics, Vol. 73, Nos. 1/2, 1988

The Bayreuth Nuclear Demagnetization Refrigerator

K. Gloos, P. Smeibidl, C. Kennedy,* A. Singsaas,† P. Sekowski, R. M. Mueller,‡ and F. Pobell

Physikalisches Institut, Universität Bayreuth, D-8580 Bayreuth, West Germany

(Received April 11, 1988)

The design, construction, and performance of a Cu nuclear refrigerator are reported. The first nuclear stage (total 275 moles Cu with 104 moles Cu in 8 T) has refrigerated a ^{195}Pt NMR thermometer in the low-field experimental region to 15 μK; it can keep experiments below 20 μK for more than 1 week. It can alternatively precool a second nuclear stage (2 moles Cu in 9 T). Demagnetizing this stage has resulted in a temperature of at most 12 μK as measured by another ^{195}Pt NMR thermometer attached to the stage. The details of the thermometry are described and possible origins of the observed internal heat leaks as well as unexpected contributions to the specific heat of the nuclear stages are discussed.

1. INTRODUCTION

At present the only method to refrigerate deeply into the microkelvin temperature range is adiabatic demagnetization of nuclear magnetic moments. After the first pioneering experiments by Kurti *et al.*,[1] Lounasmaa and co-workers[2] developed this method as a refrigeration technique for $T < 1$ mK. They were the first to use the now standard method of combining a ^{3}He-^{4}He dilution refrigerator with a superconducting magnet to achieve the required starting conditions for temperature and field to demagnetize a copper nuclear stage to a few hundred microkelvins. A further step was the double-stage nuclear refrigerator built in Jülich,[3,4] where a $PrNi_5$ nuclear stage was added between the dilution refrigerator and the copper nuclear stage to further reduce the starting temperature to demagnetize 10 moles of copper. This, as well as the chosen design, resulted in a larger entropy reduction, thereby increasing the cooling capacity, and in smaller heat leaks;

*Present address: Department of Physics, University of California, Berkeley, California 94720.
†Present address: Max Planck Institut für Physik und Astrophysik, D-8000 Munich 40, West Germany.
‡Permanent address: Kernforschungsanlage Jülich, D-5170 Jülich, West Germany.

0022-2291/88/1000-0101$06.00/0

the minimum equilibrium temperature was reduced by almost an order of magnitude to 38 μK in 1980. A similar but larger apparatus built in Tokyo reached 27 μK in 1983 with a 19-mole Cu stage.[5] A different approach has been taken by the Lancaster group, who situated the samples and thermometers together with the nuclear stage in the high-field region of the refrigerator.[6] Their interest has been mainly in refrigerating liquid helium, but in a modified version of their apparatus they were able to refrigerate a Pt NMR thermometer to 13 μK by demagnetizing three plates of 0.07 mole of Cu each.

In addition to these developments, progress had been made in the following areas, which are of importance for nuclear refrigeration:

1. Improvements in the design of ^{3}He–^{4}He dilution refrigerators[7] result in reduced starting temperature and hence enhanced entropy reduction of the magnetized copper stage.

2. An understanding of some of the origins and mechanisms for the annoying time-dependent internal heat sources,[4,8] which were troublesome in many of the earlier nuclear refrigerators, allows a reduction of heat flow to the nuclear stage and to experiments.

3. A better understanding of the performance of nuclear refrigerators could result in improved designs.

These developments led us to the conclusion that one could build a one-stage copper nuclear refrigerator which should perform at least as well as the double-stage refrigerators in Jülich and Tokyo. In addition, by adding a second stage to this apparatus, we aimed at reducing the temperature even further. In this paper we describe the design, construction, and performance of such a refrigerator, which has indeed achieved these goals and in addition has a very large refrigeration capacity for the microkelvin temperature range. The first nuclear stage (104 moles Cu in 8 T) has cooled a platinum NMR thermometer in the low-field experimental region to 15 μK, and has kept it at this temperature for more than 2 days; it can stay below 20 μK for more than 1 week. It has alternatively been used to precool the second stage (2 moles Cu) in a 9-T field to 3.5 mK. After demagnetizing this stage, a temperature of at most 12 μK has been measured by another Pt NMR thermometer attached to it. The first stage can also be used to refrigerate samples in the 9-T field into the low-microkelvin temperature range, resulting in B/T ratios of at least 10^5 T/K for polarization experiments.

2. PERIPHERALS

The refrigerator and all electronic equipment are located in a shielded room with about 120 dB damping from 100 kHz to 1 GHz, about 100 dB at

15 kHz, and about 40 dB at 1 kHz (Belling and Lee, Enfield, England). Only the pumping and gas handling system for the dilution refrigerator are situated outside of this room. The power lines into the room are filtered, and the pumping tubes, etc., are fed electrically isolated through its walls. Connecting an HP desktop computer (series 9000/220) did not influence the minimum temperature of the refrigerator. The temperature of the shielded room was kept constant to better than ±0.5°C.

The cryostat is suspended from an aluminum plate loaded with lead bricks such that the total weight of the setup is about 1.4 tons. The aluminum plate rests on three pneumatic vibration isolators (M Series, Newport Research Corp., Fountain Valley, CA), sitting on concrete pillars. This support system was built after the experience with the not quite satisfactory vibration isolation in Jülich.[3] Soft bellow sections were put into the tubing between the pumps and the refrigerator.

A seismometer[9] was used to measure vertical vibrations of the cryostat. This is not necessarily the most important mode of vibration in terms of heat leaks (for example, eddy current heating could be expected from horizontal vibrations of the nuclear stage relative to the magnet assembly). However, as it is reasonable to expect coupling between any vibrational modes present and the measured modes, we obtained a qualitative measure of the oscillations with which we could observe the effect of any improvements. The initial measurements showed that vibrations at several distinct frequencies were coming onto the cryostat. The largest oscillations were seen at 16 Hz and had an acceleration of 1 mm/sec^2 (0.1 μm amplitude). Measurements on the laboratory floor and on the pumping lines to the cryostat showed that the latter were the more probable route of transmission. Some 50% of the peaks in the vibration spectrum could be identified with the running of the pumps. By placing rubber feet on these pumps and by replacing the metallic flexible tubes in the pumping lines partly with thick-walled rubber, we were able to reduce the largest vibration amplitudes by about one order of magnitude in the frequency range 4–100 Hz.

For magnetizing the two nuclear stages we use a superconducting magnet system with 8 T and 100 mm diameter in the upper magnet and 9 T (homogeneous to 10^{-4} in a 10-mm-diameter sphere) and 50 mm diameter in the lower magnet (Fig. 1) (American Magnetics, Oak Ridge, TN). The magnets are compensated in such a way that the upper experimental region (152 mm diameter) between the dilution refrigerator and the first nuclear stage experiences 5 mT when both magnets are at their full fields. The region between the two nuclear stages is calculated to be compensated to a maximum field of 2 mT, and the field of the first magnet at the center of the second magnet was measured to be reduced by a factor of 2×10^{-3}. Rather annoying are residual fields of order 1 mT and field changes, possibly

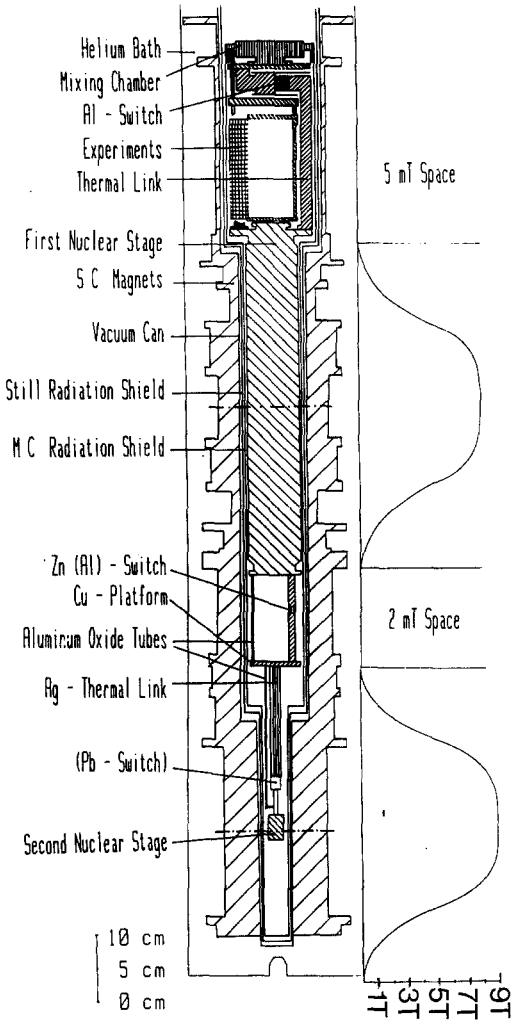

Fig. 1. Schematic of the low-temperature part of the apparatus with the two superconducting magnets and their field profile. The first nuclear stage contains 17 kg or 275 moles of copper, of which 6.6 kg or 104 moles of copper is effectively in a field of 8 T. The stage is 525 mm long with a 125-mm-diameter flange and a 78-mm-diameter body. The second nuclear stage contains 126 g or 2 moles of copper in a field of 9 T.

due to flux creep, of order 0.1 mT/day observed after demagnetization to a few mT (similar observations were made in ref. 10). The lower magnet can be used for a second nuclear stage with experiments mounted either on it (inside the high-field region) or in the compensated 2-mT region above the second nuclear stage. Or we could put an experiment instead of the second nuclear stage into the 9-T region, which is then refrigerated by the first nuclear stage only. This would allow high-polarization experiments with a B/T ratio of at least 10^5 T/K.

For precooling we use a commercial ^{3}He-^{4}He dilution refrigerator with a cooling power of 2.5 (37) μW at 10 (25) mK (SHE Corp., San Diego, CA). About 110 electrical leads and eight capillaries for liquid helium and for hydraulically actuated cold valves were heat sunk at 4 K, on the cold plate, still, base plate, and mixing chamber. The minimum temperature of the dilution refrigerator (4.5 mK) was not degraded after adding these features and after mounting the nuclear stages. We use brass for the radiation shields and for the vacuum can. Copper foils are epoxied to the mixing chamber shield to improve its thermal conductivity and to bring the temperature of its bottom end to about 20 mK. The thermal shields are centered relative to each other by nylon strings. Below the mixing chamber and thermally coupled to it is a Cu ring, to which we anchored the field coils and shields against magnetic fields which are used on experiments and thermometers mounted on top of the first nuclear stage.

3. NUCLEAR STAGES, THERMAL LINKS, AND HEAT SWITCHES

3.1. The First Nuclear Stage

The heart of the apparatus is the first nuclear stage (Fig. 2). It was melted in a high-purity graphite crucible from electrolytic copper of 6N purity (with respect to metallic elements) (Metallurgie Hoboken-Overpelt, Hoboken, Belgium). The melting was performed in a vacuum between 10^{-5} and 10^{-4} mbar; afterward the temperature was reduced to 500°C within 5 h and to room temperature within another 11 h. After casting, the copper was machined to its final shape. Thirty-six slits of 0.4 mm width were then cut electroerosively along its long axis (except at the ends, where the field has decreased to at most 50 mT) to reduce eddy current heating during the demagnetization. For annealing the stage in a ceramic oven the temperature was first increased within 30 h to 950°C and then maintained for 37 h in an O_2 atmosphere of 10^{-3} mbar and for 50 h in O_2 of 5×10^{-4} mbar (temperatures are ±30°C, depending on position along the stage). After switching off the heater, the Cu was cooled by He gas to 100°C within 11 h. This procedure resulted in very large crystallites in the nuclear stage (Fig. 2),

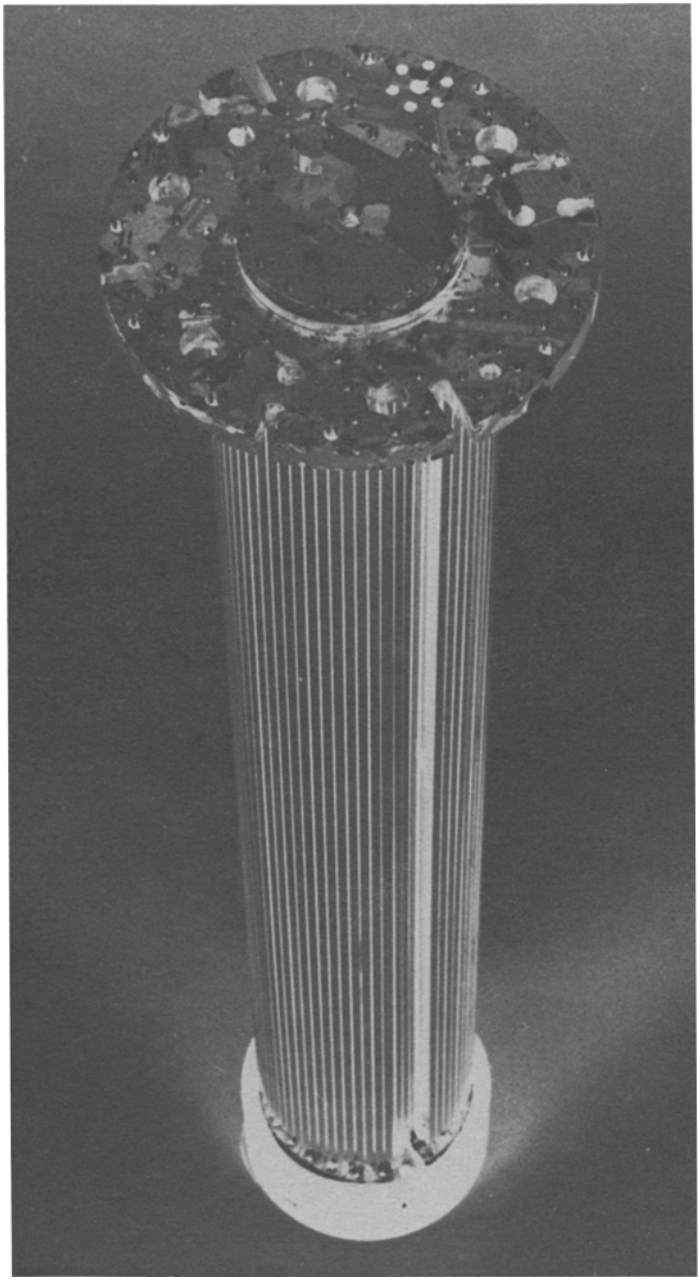

and in residual resistivity ratios of 1000 ± 500, depending on position along the stage. The upper and lower flanges were gold-plated. Since the refrigerating part of the Cu and the Cu flange, where experiments and thermometers are mounted, are cast as one complete unit, we avoid potentially high-resistance joints between them. The stage has a total length of 525 mm with a diameter of 78 mm on the main part and the lower flange, and 125 mm diameter on the upper flange. The total mass of the first nuclear stage is about 17 kg. Of these, effectively 6.6 kg or 104 moles is in a field of 8 T. Al_2O_3 wool was put into the slits to prevent vibration of the soft copper sheets.

The stage contains on its upper flange eight sites for experiments or thermometers with diameters up to 28 mm and one site for an experiment with a diameter of up to 58 mm. The height of the experiments can be up to about 160 mm. The stage is supported from the mixing chamber by three Al_2O_3 tubes of 180 mm length, 8 mm o.d. and 4 mm i.d. The total amount of organic material used on this stage is only a few milligrams.

In one of the first runs the stage was partly deformed because of a magnet quench which occurred above 8 T, and it was not annealed again. All experiments described below were carried out after this accident.

The low-temperature thermal conductivity of the first nuclear stage was measured by heating its upper flange while keeping the central high-field region at constant temperature $T_{\mathrm{Cu,el}}$. The temperature T_{Fl} of the upper flange was measured with the Pt NMR thermometer at 0.4 mK to 4 mK, and with $64\ \mathrm{mT} \leqslant B \leqslant 500\ \mathrm{mT}$ on the stage.

With a thermal conductivity $\kappa = \kappa_0 T$, the relation between heating power and temperature is

$$\dot{Q} = (A\kappa_0/2L)(T_{\mathrm{Fl}}^2 - T_{\mathrm{Cu,el}}^2) \tag{1}$$

where A is the cross-sectional area of the nuclear stage (35.6 cm^2) and L is an effective length, for which we take 26 cm (half the total length of the stage). The measured thermal conductance $(A/L)\kappa_0 T$ of our stage is $4.2T$ (W/K) or $\kappa_0 = 3.1$ (W/K^2 cm); this is about five times smaller than the calculated thermal conductivity using the Wiedemann-Franz law and the measured residual resistivity ratio of 1000. Similar deviations from the Wiedemann-Franz law of Cu nuclear stages at low temperatures have been observed previously.[4,5] We have observed these deviations for several pure metals and will report the results in a separate paper.[11]

Fig. 2. Photograph of the first nuclear stage. On the top flange one can see the large crystallites which result from annealing. The various holes are for mounting experiments and thermometers. The stage is slit, except at the flanges, to reduce eddy current heating.

3.2. The Second Nuclear Stage

The second nuclear stage was cut from 5N electrolytic copper and was annealed at 1000°C for 12 h in 2×10^{-6} mbar vacuum and for 50 h in 10^{-5} mbar O_2. The main part of this stage is a block of $20\times20\times40$ mm^3 (Fig. 3). It was cut with a saw to a design like the recent Helsinki nuclear stage[12] to reduce eddy current heating. Three $38\times15\times1.5$ mm^3 leaves extend from the top of the block to make thermal contact to the five Ag foils of the thermal link between the two nuclear stages. The total amount of copper of this stage is 126 g or 2 moles in 9 T.

For supporting the second nuclear stage, a copper platform (see below) is connected by three Al_2O_3 tubes of 8 mm o.d., 4 mm i.d., and 128.5 mm

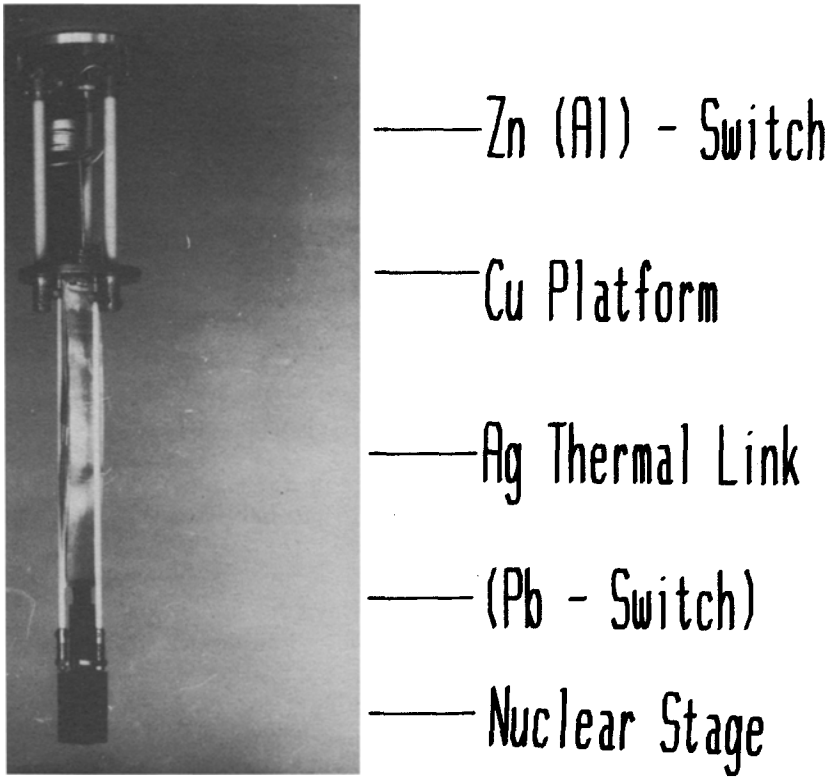

Fig. 3. Photograph of the part below the first nuclear stage. This part is bolted to the first nuclear stage (without the shown Al plate on top). It contains a Zn or Al heat switch inside of its field coil, the copper platform, the Ag thermal link, the Pb heat switch, and the second nuclear stage containing 2 moles of copper.

length to the bottom flange of the first nuclear stage. From this Cu platform three Al_2O_3 tubes of 4 mm o.d., 2 mm i.d., and 205 mm length extend down to the second nuclear stage (see Figs. 1 and 3 for this design). The total amount of organic material used on the second stage is of order 1 mg.

3.3. Thermal Link between the Dilution Refrigerator and the First Nuclear Stage

The heat switch between the dilution refrigerator and the first nuclear stage consists of 19 Al foils ($45 \times 20 \times 0.11$ mm^3) of 6N purity whose ends are gold plated.[3,13] The RRR of the Al is 2400 ± 200. At 100 mK the switch already has a thermal resistance of 3×10^6 K/W and a switching ratio of about 7×10^4 (Fig. 4). The switch sits inside of a Nb shield and is mounted horizontally below the mixing chamber (Fig. 1). The main Cu part of the link between mixing chamber and nuclear stage has a length of 230 mm and a cross-sectional area of 330 mm^2. The design involves two 90° angles and five gold-plated screw joints, which, when originally fastened with Cu screws, had resistances up to 2 $\mu\Omega$ at room temperatures. These resistances could be reduced by about an order of magnitude by putting a thin layer of Ag powder on the joining areas and by using Be-Cu screws for all joints except the one at the nuclear stage. In order to increase the pressure on

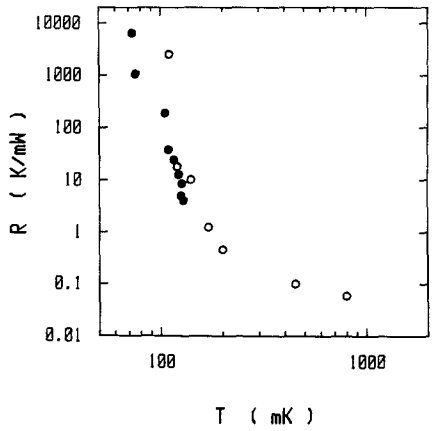

Fig. 4. Thermal resistance R of (○) the superconducting Al heat switch (19 foils of $45 \times 20 \times 0.11$ mm^3) between mixing chamber and first nuclear stage, and of (●) the superconducting Zn switch (5 foils of $30 \times 15 \times 0.1$ mm^3) between first nuclear stage bottom and Cu platform (see Figs. 1 and 3).

the joining areas after cooldown we used several 0.5-mm-thick tungsten or molybdenum washers on each joint. The electrical resistance of all press contacts between mixing chamber and nuclear stage is now 0.5 $\mu\Omega$ at room temperature. The thermal conductance of the total link measured from 6 to 50 mK is $0.24T$ (W/K), quite adequate for the cooling power of our dilution refrigerator. The thermal link between Al switch and copper flange of the nuclear stage contains 790 g (12.5 moles) Cu, 31 g Mo, and 21 g Be–Cu.

3.4. Thermal Link between the Two Nuclear Stages

We used two different designs for the thermal link between the bottom flange of the first nuclear stage and the second nuclear stage (Figs. 1 and 3). The link from the first stage to the Cu plate supporting the second stage was in both cases provided by two Cu pieces with lengths of 70 and 30 mm, and of 78 and 40 mm, respectively. At first we used a link with cross section of 1.5 cm^2 over the whole length; the two pieces in the second setup had cross sections of 7 and 5.7 cm^2, respectively. Five Zn foils ($30\times15\times0.1$ mm^3) in the first and five Al foils ($30\times20\times0.1$ mm^3) in the second setup, all with gold-plated ends, fitted into slits of the two Cu parts to join the first stage to the Cu platform. A length of 10 mm of each foil acted as a superconducting heat switch actuated by a field coil. We used tungsten washers on the Al/Cu joints to increase the pressure after cooldown. All copper parts were annealed for 50 h at 900°C in 10^{-5} mbar O_2 giving RRR between 700 and 800. At 4.2 K the electrical resistance of this path was measured to be 0.4 $\mu\Omega$ (0.1 $\mu\Omega$) for the first (second) setup. The thermal conductance between first stage and platform was $0.04T$ (W/K) [$0.2T$ (W/K)] measured between 12 and 35 mK (1.1 and 3.8 mK).

For the original setup, the thermal link from the platform to the second nuclear stage consists of five Ag foils ($180\times30\times0.5$ mm^3). The foils had a purity of 5N and were annealed for 20 h at 900°C in 10^{-5} mbar O_2. Their lower ends join to a Pb heat switch ($10\times20\times1$ mm^3) bolted to the Cu sheets of the upper end of the second nuclear stage (Figs. 1 and 3). This lower heat switch is actuated by the field of the 9-T magnet, of which it experiences about 94%. For calibration of the Pt NMR thermometer on the second stage, the Pb switch was replaced by a Ag foil. The electrical resistance at 4.2 K between Cu platform and second stage is about 0.8 $\mu\Omega$. The thermal conductance between Cu platform and second nuclear stage is $0.04T$ (W/K), measured between 18 and 35 mK. There are eight screw joints along the thermal path between the two nuclear stages.

For the second setup we used the same silver foils as before, shortened to $169\times30\times0.5$ mm^3. The electrical resistance at 4.2 K between Cu platform and second stage is now about 0.2 $\mu\Omega$. The thermal conductance between

Cu platform and second nuclear stage deteriorated after some cooldowns and eventually reached $0.03T$ (W/K), measured from 4 to 10 mK. There are five screw joints along the thermal path between the two nuclear stages.

The link between the Zn (Al) switch and the second stage contains 241 g (3.8 moles) Cu, 134 g (1.2 moles) Ag, 6 g BeCu, 7 g W, and 2 g Pb for the first design, and 430 g (6.8 moles) Cu, 125 g (1.2 moles) Ag, and 0.5 g W for the second design.

4. THERMOMETRY

4.1. Calibration

Our thermometry depends on calibration between 15.6 and 208 mK using a superconducting fixed-point device from the National Bureau of Standards (model SFPD SRM 768), which is mounted on the bottom plate of the mixing chamber of our dilution refrigerator. It is shielded from magnetic fields by a superconducting niobium cylinder surrounded by a

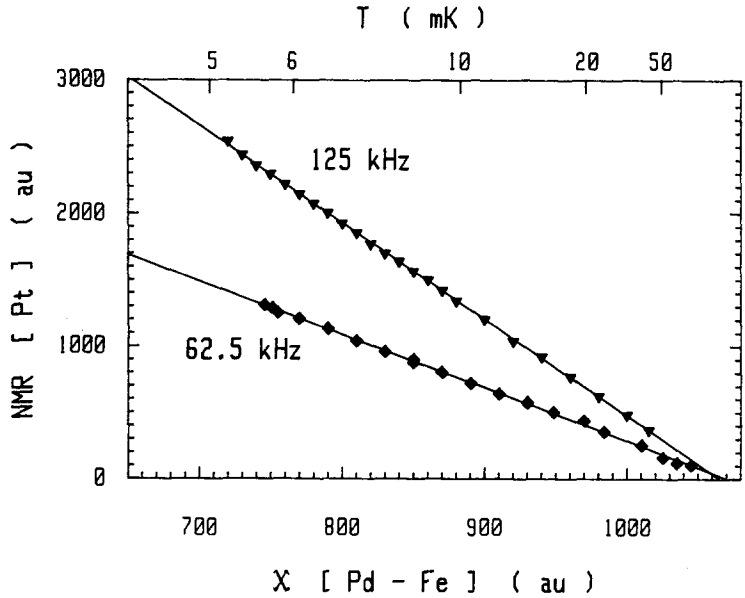

Fig. 5. NMR signal from the platinum NMR thermometer on the first nuclear stage, measured at the two indicated frequencies, versus susceptibility signal from the $Pd+11$ ppm Fe thermometer which is mounted on the bottom of the mixing chamber. The temperature scale is given on the top horizontal axis.

soft magnetic shield (Cryoperm 10, Vakuumschmelze, Hanau, West Germany), both closed at one end; the latter is degaussed just above 10 K. With the fixed-point device we calibrate the resistance of 0.1-mm-thick carbon thermometers as well as the susceptibility of a (*Pd* + 11 ppm Fe) thermometer,[14,*] which is also mounted on the bottom plate of the mixing chamber; its calibration is very reproducible from run to run. The (*Pd* + 11 ppm Fe) thermometer is used to calibrate the NMR thermometers between 5 and 100 mK (see below and Fig. 5).

4.2. Platinum NMR Thermometry

On the first nuclear stage and on the platform between the first and the second stages we have Pt NMR thermometers of the Jülich design.[3,15] These thermometers contain about 3000 Pt wires of 25 μm diameter (Johnson Matthey, Royston, Herts., England) with a thin layer of SiO_2 evaporated onto them for insulation. One end of the wires is welded to a $22 \times 3.7 \times 2$ mm^3 Pt plate, which is bolted with Ag screws to an $80\,(60) \times 4 \times 3$ mm^3 Ag cold finger, which is then bolted to the top flange of the first nuclear stage (platform). These Pt thermometers and their field coils sit inside Nb shields. The field coils and shields on the thermometers have no thermal contact to their nuclear stage, but are heat sunk to the refrigeration stage above it.

The thermometer on the second stage is of similar design, but its Pt plate ($11 \times 3.7 \times 2$ mm^3) has a 3-mm thread at its end and is screwed directly into the lower end of the Cu body of the second stage. This thermometer was used for the results shown in Figs. 14 and 15. For the results shown in Fig. 13 we used an earlier version of a Pt wire thermometer. It was constructed from 800 Pt wires of 25 μm diameter (Johnson Matthey), which were melted into a sphere of silver of approximately 3 mm diameter. A 400-Å layer of SiO was evaporated onto the Pt wires for insulation. The silver sphere was spot welded to a 10-mm-long Cu stem, which was then screwed into the second nuclear stage. The NMR field for the thermometer on the second nuclear stage is provided by the 9-T magnet after demagnetization of the stage; the measurements were affected by field changes, possibly from flux creep, of order 0.1 mT/day after demagnetization to the NMR field.

The transmitter/receiver signal coils for all Pt NMR thermometers are made from 25-μm insulated Cu wire with RRR = 76 and have the following dimensions: length 4–5 mm, diameter 2.2–2.7 mm, number of layers 6–10,

*Recently, we have used commercial "pure" Pd for our thermometry, which contains 15 ppm Fe, <1 ppm Co, 1 ppm Ni, and 2 ppm Cr (Demelloy 99.99%, Demetron, Hanau, West Germany).

number of turns 750–1300. The Cu Wire is wound onto a 6-μm-thick Mylar coil former and fixed with a very tiny amount of diluted GE varnish. The coil is then pushed over the Pt wire bundle and fixed there also with diluted GE varnish. The twisted leads to each coil are heat sunk at the Ag coldfingers. By heating the signal coil, we determined the conductance from the coil/Pt thermometer combination to the nuclear stages as $0.02T$ ($0.14T$) (W/K) at 50–80 (15–30) μK for the first-stage thermometer (second version of second-stage thermometer). These conductances make the influence of direct thermal leaks to the Pt thermometers via the signal coils unlikely. This was also confirmed by using an equivalent thermometer with a free-standing signal coil on the first stage, which indicated the same temperatures.

For the pulsed NMR electronics we use an instrument similar to the commercial PLM3 (Instruments for Technology, Espoo, Finland), operating at 62.5 kHz (or 125 kHz at higher T). The signal coils are tuned outside of the cryostat to a quality factor of 3–5. The signal-to-noise ratio of the Pt thermometers is 1 at about 150 mK.

We use a pulse length of typically 0.5 msec duration to give maximum NMR amplitude at $T \geqslant 0.25$ mK, especially for calibration. At the lowest temperatures the excitation amplitude was reduced by about a factor of 10, which results in less than 0.1 nJ total heat per pulse. Between the pulses we wait for several time constants τ_1 of Pt. The waiting times were changed between 15 min and 2 h at our lowest temperatures without influence on the results, demonstrating that the rf pulses had no effect on the indicated temperatures. Influences from the NMR electronics were checked by disconnecting and shielding the leads to the rf coil between pulses.

The chosen settings of our NMR electronics together with the relaxation times and thermal conductances of our Pt thermometers make the potential problems in low-temperature NMR thermometry discussed recently by Eska[16] negligible.

A confirmation of our temperature calibration, at least for $100\ \mu\text{K} \leqslant T \leqslant 100$ mK, came from two observations. First we found that the electronic susceptibility measured for our $Pd+11$ ppm Fe sample is proportional to the nuclear magnetization of the platinum wires in the NMR thermometer to within a few tenths of a percent in the investigated temperature range 5–100 mK (Fig. 5). In addition, we observe that the B/T ratio for the field on the first nuclear stage and the temperature from its Pt thermometer stayed constant from the starting conditions, 8 T and 10 mK, to at least 80 mT and 100 μK, within 3% (see Fig. 9). From these observations and from the experience of more than ten cooldowns we believe that our thermometry is correct to about 5% at 15 μK and to about 2% at 1 mK (assuming the NBS fixed-point temperatures to be correct, National Bureau of Standards, model SFPD SRM 768).

4.3. Korringa Relation of the Pt NMR Thermometers

In Refs. 2 and 17–19 it was observed that the Korringa constant κ of Pt powder is temperature and field dependent at $T \leq 30$ mK and $B < 30$ mT. This was explained in ref. 20 as resulting from the influence of magnetic impurities at the ppm level, in particular Mn forming a Kondo state in Pt with $T_K \simeq 0.01$ K.[21] A drastic reduction of τ_1 due to magnetic impurities has also been observed for Cu at submillikelvin temperatures and at $B < 10$ mT.[22]

Whereas in refs. 2 and 17–19, κ of Pt powder changed at most by a factor of 2 for $1.3 \leq T \leq 30$ mK and $5.7 \leq B < 30$ mT, we observe almost an order-of-magnitude change of κ for the 25-μm Pt wires in the thermometer on the first nuclear stage at $T < 10$ mK when we decrease the field from 27 to 6.8 mT (Fig. 6).

According to the supplier, the starting Pt is of 5N purity (Johnson Matthey), and we measure RRR of about 400 after annealing it at 900–1000°C in about 4×10^{-3} mbar air, but the Pt wires of the thermometer were annealed for several hours after SiO was evaporated onto them.[15] Only later did we learn that this treatment severely reduces the electrical conductivity of the wires to an RRR of about 20 (Fig. 7). On the other hand, the data

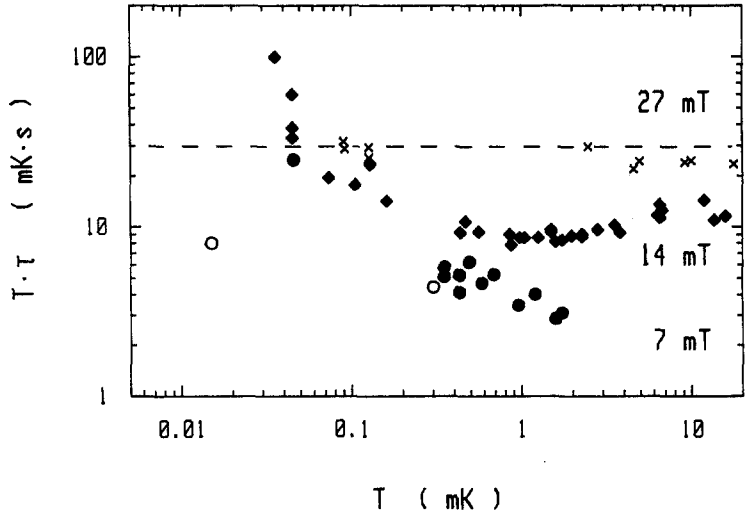

Fig. 6. Temperature T multiplied by time constant τ of the platinum NMR thermometers measured in the three indicated magnetic fields. (- -) The high-field, high-temperature value $\kappa = 30$ mK sec for the Korringa constant of Pt. The increase of $T\tau$ at $T < 0.2$ mK is caused by the thermal time constant. (○) Results for the thermometer on the second nuclear stage, which has a higher conductance than the thermometers on the first nuclear stage and on the platform for which the other data were taken.

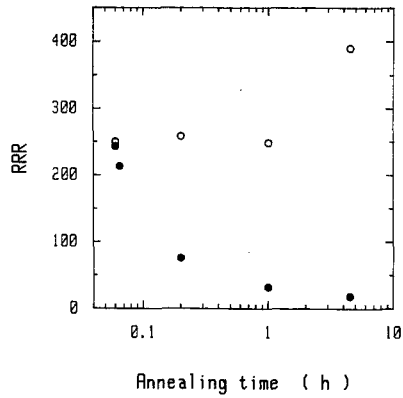

Fig. 7. Residual resistivity ratio of the 25-μm Pt wires of the NMR thermometers after annealing at 900°C in about 6×10^{-3} mbar air (●) with and (○) without SiO evaporated onto them before annealing.

in Fig. 6 demonstrate that these Pt NMR thermometers have rather short relaxation times; the best values for the spin lattice plus thermal relaxation times at 7 mT are 4 sec at 1 mK and 9 min at 15 μK, respectively (see also Fig. 15).

It is important to emphasize that the behavior of the Korringa constant and the low RRR did not result in a deviation of the nuclear magnetization of our Pt from a Curie law (see Section 4.2), at least at $T \geqslant 100\ \mu$K, in agreement with the Jülich results for similar Pt wires.[3]

The effective spin-spin relaxation time of our Pt thermometers is between 0.46 and 0.82 msec.

5. PERFORMANCE OF THE NUCLEAR REFRIGERATOR

For the measurements described here, we mounted only heaters of Pt-W wire (25 μm diameter, several centimeters in length) and the various thermometers on the nuclear stages. All leads to these devices are superconducting between mixing chamber and nuclear stages, and they were carefully heat sunk.

5.1. Precooling by the Dilution Refrigerator

The precooling of the magnetized first nuclear stage is shown in Fig. 8. The temperature-time dependence is $T \propto t^{-1/3}$. This is the expected behavior as long as the cooling power of the dilution refrigerator varies as T^2 and the specific heat of the nuclear stage varies as T^{-2} and they are connected by a metallic link.

The first nuclear stage in a field of 8 T reaches 15 mK (12, 10 mK) after 18 h (35, 70 h) precooling. This corresponds to an entropy reduction of

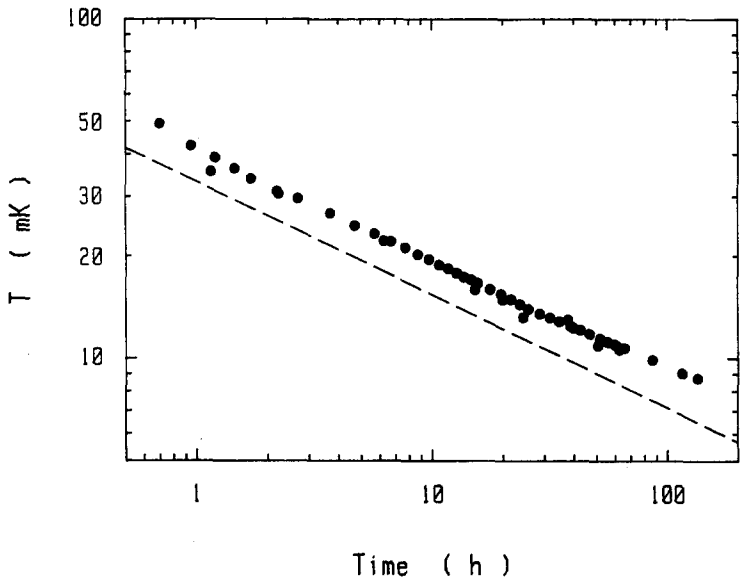

Fig. 8. Precooling of the magnetized first nuclear stage by the dilution refrigerator as a function of time. The dashed line represents $T \propto t^{-1/3}$ for comparison (see text).

about 4% (6, 8%) of our 104-mole Cu stage. After opening the heat switch to the nuclear stage, the dilution refrigerator again reaches 4.5 mK.

5.2. Performance of the First Nuclear Stage

5.2.1. Minimum Temperature

After having achieved a desired starting temperature of about 10 mK, the first nuclear stage is demagnetized by reducing the field in steps by a factor of 2 to a final field of a few mT. The sweep rate was 2 T/h at $B \geq 0.5$ T and was then stepwise decreased by a factor of 2 proportional to the field. Between each step we wait for thermal equilibrium and measure the temperature. Some results for demagnetization of the first stage without the second stage connected to it are shown in Figs. 9 and 10.

The data in Fig. 9 demonstrate that we did not see any nonadiabaticity of the demagnetization to within less than 3% to a temperature of 100 μK. The minimum temperature at $B_f = 2$ mT measured with the Pt NMR thermometer was 15 μK (±5%); at 4 mT the minimum temperature was almost identical (Fig. 10). This is the lowest equilibrium temperature measured in a low-field region. We saw no change of the minimum temperature for 50 h after demagnetization to within a scatter of ±1% of the NMR reading.

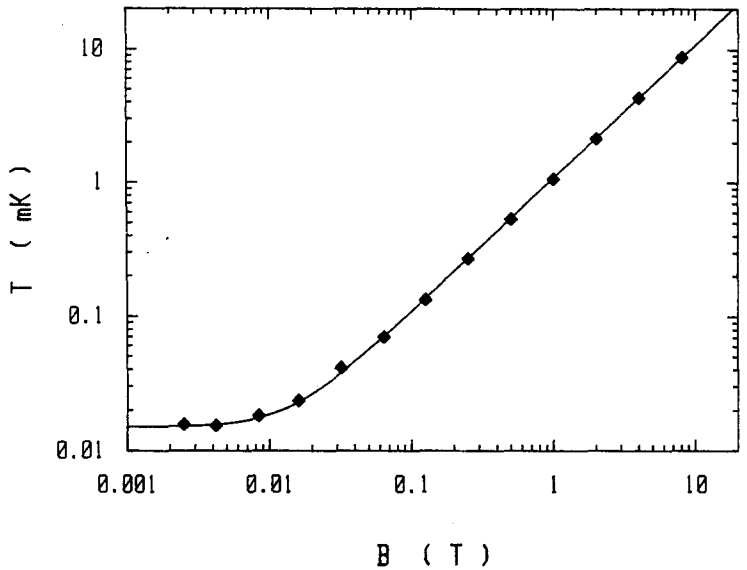

Fig. 9. Temperature measured by the pulsed Pt NMR thermometer in the experimental region of the first nuclear stage as a function of the field applied to the first nuclear stage. The demagnetization behaves in an ideally adiabatic way to at least 100 μK. The deviation at lower temperatures is caused by temperature gradients between the center of the nuclear stage and Pt thermometer. (—) The behavior of the temperature of the Pt thermometer calculated with $T^2 = (T_i B/B_i)^2 + (15\ \mu\text{K})^2$.

These results were obtained about 4 weeks after cooldown of the apparatus. The heat capacity of the first nuclear stage should be large enough to keep the temperature below 20 μK for more than 1 week.

In the early runs we had a Cu foot on the Pt NMR thermometer. A substantial fraction of this foot sees the field applied to the Pt NMR thermometer. It soon became obvious that for this set-up the relaxation time and the minimum temperature were limited by the large parasitic nuclear specific heat of this copper foot. This is demonstrated by the results shown in Fig. 10 for two different NMR fields, 13.7 and 6.8 mT, with the Cu foot, and results with an NMR field of 6.8 mT with an Ag foot on our thermometer, to which we eventually changed the design.

The slowest part in the path from Cu nuclei in the stage to Pt nuclei in this thermometer is now the *thermal* time constant of the Pt nuclei exposed to the 7-mT NMR field. This response time is about 1 h at 15 μK.

From the experience with our present thermometers it seems that the minimum temperature and the slow relaxation in the Jülich refrigerator[3] result at least partly from using Cu instead of Ag for the thermometer foot.

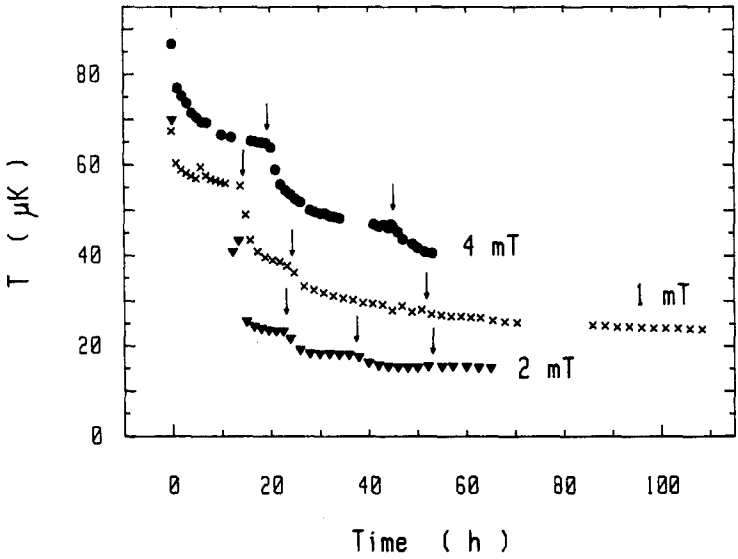

Fig. 10. Temperature measured by the Pt NMR thermometer on top of the first nuclear stage as a function of time for the last few demagnetization steps. The measurements were performed at (●) 13.7 mT with a Cu foot on the Pt thermometer; (×) at 6.8 mT with a Cu foot; (▼) at 6.8 mT with a Ag foot. At the arrows the field was decreased by a factor of 2; the final fields are given for each demagnetization.

5.2.2. Heat Leaks

The heat leak to the first nuclear stage was determined by various methods, which will be described in this section.

The optimum final demagnetization field of 2–4 mT (Figs. 9 and 10) gives as a first rough estimate a total heat leak of about 2 nW to the stage.

Heat leaks at low temperatures and small fields measured by the remagnetization method (here remagnetization to 0.5 T) after letting the stage sit at its final temperature and field for 1–2 days[3] are rather uncertain at our final fields, because of possible residual fields of order 1 mT and field changes due to flux creep (see Section 2) of the main superconducting magnets. In addition, losses caused by nonadiabaticity in the de- and remagnetizations cannot be separated. Thus, the heat leak of about 1.5 nW measured by this method at least 10 days after cooldown is again only a "first guess" for the heat leak on the first nuclear stage.

The most reliable method to determine $\dot{Q}$ is to observe the drift of temperature versus time at $10 \leqslant T \leqslant 30$ mK and no magnetic field applied to the nuclear stage, i.e., under conditions of negligible temperature gradients and well-known small specific heat. Figure 11 shows the heat leak

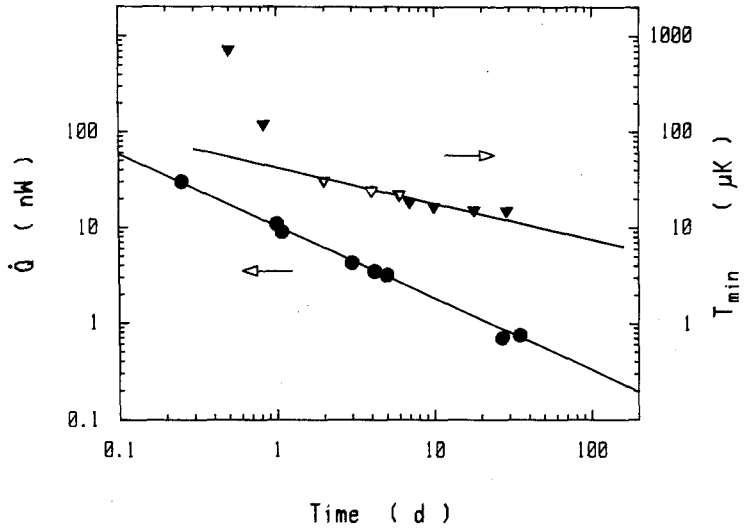

Fig. 11. Left scale: (●) Heat leak as a function of time after reaching 4 K for the first nuclear stage. The values for $\dot{Q}$ were determined in various runs from the warmup rate at $10 < T < 30$ mK and with no field on the stage. The line is $\dot{Q} \propto t^{-3/4}$. Right scale: (▼) Minimum temperature measured by Pt NMR thermometry on top of the first nuclear stage as a function of time after reaching 4 K. (▽) Data taken as a function of time after warming to 1 K; the apparatus had been well below 4 K for several more days. The line is the temperature calculated with the model discussed in the text.

measured for the first nuclear stage by this method as a function of time after cooling to 4 K. These measurements show that the heat leak is only 10 nW already 1 day after cooldown and has decayed to 1 nW after 3 weeks of operation below 4 K. This latter value is the same value as the heat leak in the Jülich refrigerator, which contained a ten times smaller copper stage.[3,4] In addition, the time dependence $\dot{Q} \sim t^{-3/4}$ is much weaker.

This "high-temperature" heat leak is not necessarily identical to the "low-temperature" heat leak at the final temperatures and fields. This is demonstrated by the heat leak values obtained from the temperature drift during various specific heat measurements at $B = 2$, 5, and 6 mT and $0.15 < T < 10$ mK. It resulted in $\dot{Q} \simeq 0.4$ nW at $T \ll 1$ mK and $t > 10$ days. These measurements showed an unexpected temperature-dependent contribution to the heat leak (Fig. 12), which may indicate that under these measuring conditions we are "running" against the energy reservoir of the excess specific heat at $T \simeq 0.5$ mK (see Figs. 16-18 and Section 4.5).

With known heat leaks and thermal conductances we can calculate the temperature distribution in our apparatus. For this calculation we assume a molar heat leak of $\dot{q} = \dot{Q}/N$, independent of the metal involved, where

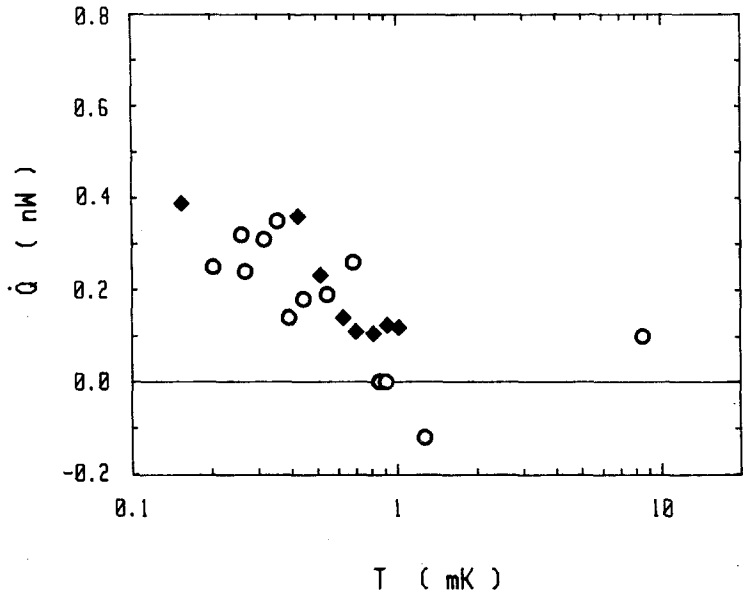

Fig. 12. Heat leak to the first nuclear stage determined during the specific heat measurements whose data are shown in Fig. 16 as a function of temperature. The data are taken with (◆) 5 mT and (○) 2 mT on the first nuclear stage.

$\dot{Q}$ is the measured total heat leak and $N = 275$ moles, the total number of moles.

With the starting conditions $T_i/B_i = 10\,\mathrm{mK}/8\,\mathrm{T}$, and assuming adiabaticity, the nuclear temperature of the $N_0 = 104$ moles of Cu in the high-field region is T_iB/B_i, and their electrons are at

$$T_{\mathrm{Cu,el}} = (T_iB/B_i)(1 + \kappa\dot{q}N/\lambda N_0B^2) \tag{2}$$

The Korringa and Curie constants of Cu are $\kappa = 1.2\,\mathrm{K\,sec}$ and $\lambda = 3.19 \times 10^{-6}\,\mathrm{J\,K/mole\,T^2}$, respectively. The heat leak from the $N_1 \simeq 70$ moles of Cu between high-field region and flange and from the $N_2 \simeq 30$ moles on the flange (including thermal link and connecting parts) then produces a temperature gradient between flange and center because of the finite thermal conductance of the stage of $\beta = 4.2\,\mathrm{W/K^2}$; thus

$$T_{\mathrm{Fl}}^2 = T_{\mathrm{Cu,el}}^2 + \dot{q}(N_1 + 2N_2)/\beta \tag{3}$$

At the *optimum* final demagnetization field, Eqs. (2) and (3) give

$$T_{\mathrm{Fl}}^2 \simeq (6 + 17 + 14)\dot{q} \tag{4}$$

Correspondingly, we have with 0.1 mole and 0.02 W/K^2 for the thermometer

$$T_{Pt}^2 \simeq T_{Fl}^2 + 5\dot{q} \tag{5}$$

With this model the temperature gradient in the thermometer is only 7% at the lowest temperatures (or about 1 μK at 15 μK), and the difference between $T_{Cu,el}$ and the temperature measured by the Pt thermometer must be mainly attributed to a temperature gradient between the center of the stage and its flange.

A calculation of T_{Pt} using the measured "high-temperature" heat leak shown in Fig. 11 shows good agreement with the measured minimum temperatures (Fig. 11), confirming again our temperature scale and our interpretation of a homogeneous heat leak in the stage. The deviations from $T_{Pt} \propto \dot{Q}^{1/2} \propto t^{-3/8}$ at the lowest temperatures may result from a time-independent background of order 1 pW/mole or from a constant heat flow of about 0.1 nW to the flange.

The observation that the minimum temperature of $T_{Pt} = 15$ μK stayed constant to within $\pm 1\%$ for at least 50 h may result from the rather large temperature gradient between the slowly warming demagnetized center of the stage and its flange, and from the further decay of the heat leak during this time.

The above discussion demonstrates that the minimum temperature is not limited by the cooling capacity of the Cu nuclei or by a temperature gradient in the Pt thermometer, but by the "weak" thermal contact between the cold electrons in the high-field region (about 5 μK) and the flange of the Cu stage. Improvements are only possible by further increasing the low-temperature thermal conductivity of metals and/or further reducing heat leaks. We discuss possible origins of internal heat leaks in Section 6.

5.3. Performance of the Second Nuclear Stage

For a double-stage demagnetization, both magnetized stages (8 T/9 T on first/second stage) are precooled by the dilution refrigerator to a temperature between 11 and 12 mK. Then the upper Al heat switch is opened and the first nuclear stage is demagnetized in steps of a factor of 2 from 8 to 1 T as described in Section 5.2. After 30 h (50 h) the temperatures are 1.7 and 2.1 mK on the first stage and on the Cu platform, respectively, and about 4.5 mK (3.5 mK, which is close to the maximum of the nuclear specific heat of Cu in 9 T) on the second stage. The long thermal relaxation time and the rather high temperature of the second stage result from the weak thermal contact between platform and second stage (see Section 3.4). This weak link as well as an unexpected heat reservoir in the parts between first and second stages (see below) dictated the demagnetization procedure of

the second stage. The heat switch between platform and first stage was kept closed and the field on the first stage was decreased by a factor of 2 before the same step was taken on the field of the second stage. This assured that $T_{\text{first}} < T_{\text{platform}}$, so that as much as possible of the energy from the mentioned heat reservoir flows to the first and not to the second stage.

After precooling the second stage, the first stage in 8 mT reached minimum temperatures of 30-35 μK, indicating that the first stage still is a rather powerful refrigerant, even after precooling the second stage.

In the following we describe the demagnetization of the second stage with the two designs of the link between the two stages (see Section 3.4) and of the Pt NMR thermometer on the second stage (see Section 4.2).

With the *first designs*, the first and second stages are demagnetized to 40 and 14 mT, respectively. This resulted in 125 μK on the first stage and 140 μK on the Cu platform. The Pb switch opened at a field of about 80 mT on the second stage. Unfortunately, it remained "leaky", probably because of frozen-in flux, resulting in the heat leak given below.

Without waiting for thermal equilibrium in the second stage, we then demagnetized this stage to 7 mT. The temperatures measured by the Pt thermometer of the first design are shown in Fig. 13. Possibly due to the slow relaxation of this thermometer, the minimum temperature of 12 μK is reached only 30 h after finishing the demagnetization.

The temperature scale on Fig. 13 was obtained via two different procedures. First, in a preceding run with the Pb switch replaced by a Ag foil, the Pt NMR thermometer was calibrated with the other thermometers on the refrigerator. Second, we performed the specific heat measurements indicated in Fig. 13, which give us the nuclear temperatures T_n of the Cu stage. With the heat leak $\dot{Q}_{\text{2nd stage}} = 0.11$ nW determined from the temperature drift, we then obtain the electronic temperature $T_{\text{Cu,el}}$. Eventually, assuming a constant heat leak into the thermometers, we obtain T_{Pt} from a fit to the data. It is very gratifying that T_{Pt} determined by these two quite different procedures agreed well. The data in Fig. 13 demonstrate that the nuclear temperature right after demagnetization was 4.3 μK, in comparison to the ideal value 2.7 μK. When the Pt thermometer has relaxed to its measured minimum value of 12 μK, we have $T_{\text{Cu,el}} = 8$ μK and $T_{\text{Cu},n} = 6$ μK on the second Cu stage.

The heat leak $\dot{Q} = 0.11$ nW determined from the warmup rate during the specific heat measurements shown in Fig. 13 was determined at $T_{\text{platform}} =$ 140 μK, $T_{\text{Pt}} \leqslant 50$ μK, and at about 10 days after cooldown. This heat leak decreased to $\dot{Q} = 0.02$ nW at $T_{\text{platform}} = 187$-$256$ μK and $T_{\text{Pt}} = 118$-180 μK when the Zn heat switch to the first stage was opened. This indicates a temperature dependence of the heat leak to the second stage as well, possibly resulting from the excess specific heat with a maximum at 0.5 mK (see

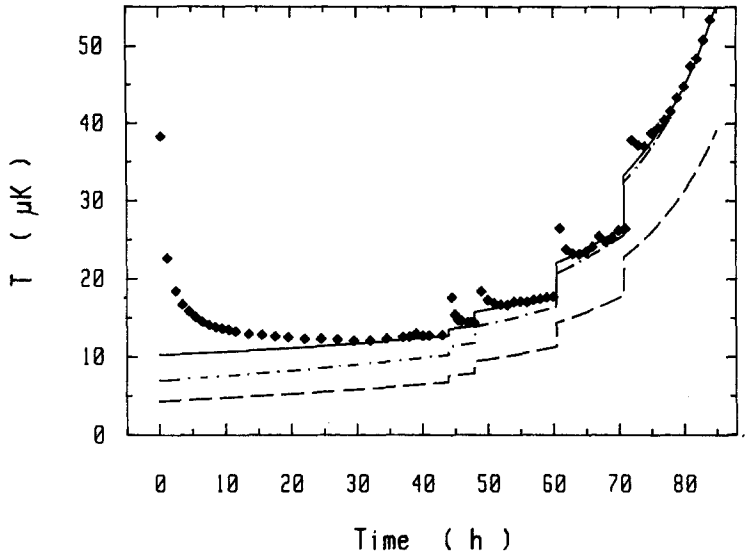

Fig. 13. Temperature T_{Pt} measured by the Pt NMR thermometer on the second Cu nuclear stage as a function of time after demagnetizing to 7 mT. The dashed line is the nuclear temperature $T_{Cu,n}$ of the second nuclear stage calculated from the specific heat measurements where the temperature of the stage was increased by applying heat as shown; it starts at $T_{Cu,n}(0) = 4.3\ \mu K$. From $T_{Cu,n}$ and from heat leak $\dot{Q} = 0.11$ nW (obtained from the warmup rate) we calculate the electronic temperature $T_{Cu,el}$ of the Cu stage shown by the dot-dashed line. The temperature of the Pt NMR thermometer is then obtained with the assumption that at $T > 40\ \mu K$, $T_{Pt} = T_{Cu,el}$.

below). Another value, $\dot{Q} = 0.12$ nW, is obtained from observing the second stage and platform drift together at a substantially higher temperature, 9–33 mK, with a field of 0.125 T on the second stage.

With the *second versions* of the thermal link and Pt thermometer, the second stage was demagnetized to 13.7 mT and left there until its temperature was constant. The resulting temperatures with a minimum value of 10–11 μK are shown in Fig. 14. Unfortunately, these values are rather uncertain (±20%) because in this field the thermometer calibration was not performed very carefully. The temperatures after the following demagnetizations of the stage to 6.8 mT are shown in Fig. 15, with a minimum value of 12 μK (±1 μK).

Even though the thermometer calibration at 13.7 mT was not performed as carefully as it was done at 6.8 mT, our data certainly indicate that the decrease of the field to 6.8 mT at least does not further decrease the temperature indicated by the second-stage thermometer (just as the decrease of the field from 4 to 2 mT on the first stage did not decrease its temperature;

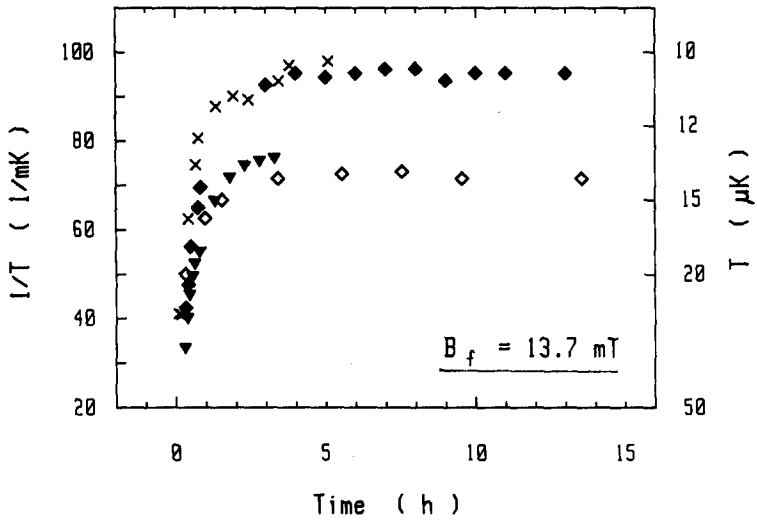

Fig. 14. Temperatures measured by the Pt NMR thermometer at 125 kHz on the second nuclear Cu stage after demagnetizing this stage to 13.7 mT. The data are from four demagnetizations in one run.

see Section 5.2). This observation seems reasonable, because 6.8 mT may already be below the optimum final demagnetization field of the second stage.

With the second version of the platform and thermal link between the nuclear stages (see Section 3.4), the platform never cooled below 70 μK even with a closed Al heat switch to the first nuclear stage at 35 μK. This observation gives a leak of 0.4 nW flowing to the first stage. With the Al heat switch to the first stage open, we can determine the heat flowing to the second stage from the temperature difference between platform and second stage, if we assume that the heat is coming from the platform (but see below). From various determinations at $T_{Pt} = 15$-163 μK and $T_{platform} = 90$-120 μK, we find values between 0.1 and 0.6 nW. From the observation that the Cu nuclei must have stayed below about 12 μK for more than 1 day we find $\dot{Q} < 0.6$ nW.

The data in Figs. 13-15 show a very fast relaxation for the second design of the Pt thermometer, which agrees with the calculated thermal relaxation times. The fast response of the Pt NMR thermometer (9 min at 15 μK, for example) was checked by applying a large rf pulse or by rapidly changing the field to cause some eddy current heating on the stage. It is remarkable that these latter relaxations occur faster than the relaxation after the original demagnetization. Another remarkable observation seems to be

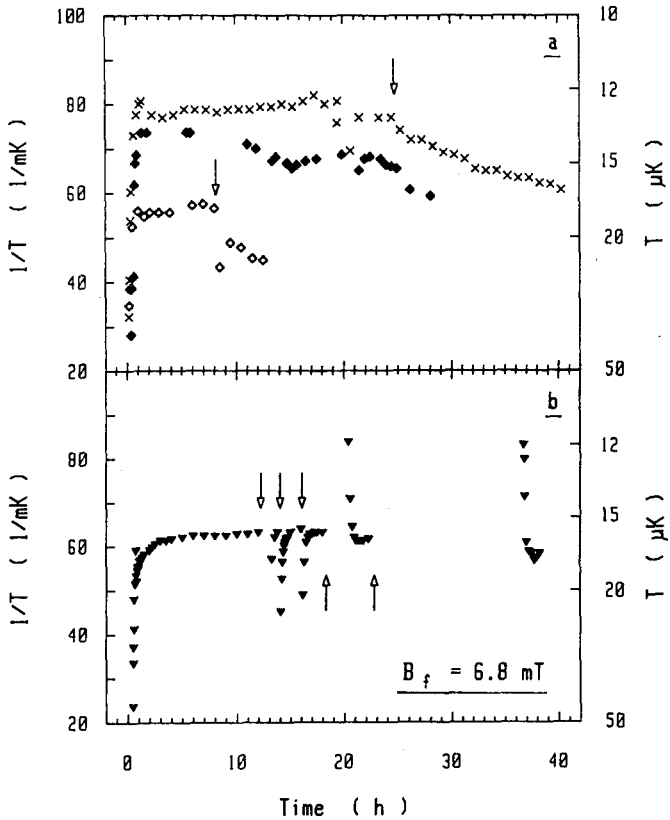

Fig. 15. Temperatures measured by the Pt NMR thermometer at 62.5 kHz on the second nuclear Cu stage after demagnetizing this stage to 6.8 mT. The data are from four demagnetizations in one run (symbols as in Fig. 14). (a) The arrows mark the time at which the heat switch to the first nuclear stage was opened. The scatter of the data (×) at 21 h is caused by a check of the NMR resonance frequency. (b) Two large rf pulses were applied to the Pt NMR thermometer and an eddy current heat pulse to the nuclear stage, as indicated by the first three arrows. At the last two arrows the field on the nuclear stage and on the thermometer was increased from 6.8 to 13.7 mT and kept there for the times where no data points are shown. It was then decreased to 6.8 mT again. Notice the overshooting of the temperature indicated by the NMR thermometer to lower values. Such an overshoot to lower T was also seen immediately after the original demagnetizations, but with a smaller amplitude. The relaxation after changing the experimental conditions occurs with a time constant of only about 9 min in 6.8 mT.

that, when the field was increased to 13.7 mT and then decreased to 6.8 mT again, the Pt nuclei first cool to a lower temperature but then decrease to the former equilibrium value; this lower temperature was also not observed after the original demagnetization (see Fig. 15).

The limitation for the final temperatures indicated by the Pt thermometer cannot be caused by too long relaxation times, as Figs. 14 and 15 indicate, but may result from the following three sources:

1. There is a heat leak of $\dot{Q} \simeq 0.5$ nW to the second stage, keeping its electrons at a high temperature while the nuclei sit at 3–4 μK. This reservoir has to sit *between* platform and second stage because otherwise the temperature of the platform would have to be larger than the measured values indicate. Such a large heat leak is about the upper limit compatible with the observation that the nuclei in 6.8 mT stay below 12 μK for more than 1 day. The heat leak evolving from the slowly relaxing Ag nuclei in the thermal link is much too small to explain such a heat leak.

2. Another explanation might be a heat leak in the Pt thermometers. If we assume that the total heat leak to the second stage comes from the platform, we find $\dot{Q} \simeq 0.1$ nW and $T_{\mathrm{Cu,el}} \simeq 5\ \mu$K. To explain the difference from the observed T_{Pt}, we need a heat heak of several pW in or to the Pt. As discussed in Section 4.2, direct thermal heating from the NMR signal coils is unlikely. We can also exclude vibration-induced eddy current heating from the NMR field as an essential source, because we see similar minimum temperatures at 6.8 and 13.7 mT on the second-stage thermometer. The temperature was also not changed by changing the time between rf pulses or by disconnecting and shielding the leads to the rf coil between pulses (see Section 4.2). More likely is the existence of internal heat leaks in the Pt wires and thermometer stem, possibly of the same origin as the heat leaks evolving from Cu in the nuclear stages. But a leak of several pW would correspond to 0.1–1 nW/mole and is about 2 orders of magnitude higher than the molar heat leak evolving from the Cu in the first stage, but not too much higher than the molar heat leak of the second stage plus platform. Since the thermal conductance of the second-stage thermometer (second version) is a factor of 7 larger than that of the first-stage thermometer, we would expect such a problem to be less significant for the second-stage thermometer, because we found a large temperature gradient quite unlikely for the first-stage thermometer (see Section 5.2.2).

3. Last but not least, we want to mention another, possibly even remoter explanation of the minimum temperatures as resulting from the approach to an ordering process, possibly nuclear magnetic ordering in our Pt samples (without internal interaction, the deviation from Curie law behavior is less than 1% for ^{195}Pt in 6.8 mT at $T > 10\ \mu$K). Such an interpretation may

receive support from the observation that the minimum temperatures measured on our first and second nuclear stages (as well as the temperature measured at Lancaster with a Pt NMR thermometer of very different design[6]) are all between 10 and 15 μK. The approach to an ordering transition may also explain the overshoot in minimum nuclear temperature (or in nuclear polarization) of the Pt which we see immediately after demagnetization and before it relaxes to equilibrium (Fig. 15). The irreproducibility observed for this behavior in different demagnetizations may indicate that the Pt nuclei are pulled by the magnetic field into a metastable state as has been observed in the Helsinki experiments on Cu.[22] The details of this behavior would then indeed depend on the starting conditions and the demagnetization schedule. Such an interpretation would require a nuclear magnetic ordering temperature about an order of magnitude higher than present approximate estimates indicate for isotopically pure ^{195}Pt,[23] but these estimates are rather uncertain due to the non-*s*-wave character of conduction electrons in the strongly exchange-dominated, high-Z metal Pt with its large negative Knight shift. Our Pt samples show a Korringa constant (electron-nuclear coupling) which is an order of magnitude lower (stronger) than the value of ideally pure Pt (Fig. 6). This may result in a correspondingly higher transition temperature. On the other hand, the observed rather fast thermal relaxation of the Pt thermometers gives no hint for an increasing specific heat expected if an ordering transition is being approached.

An alternative type of ordering could, of course, be spin-glass freezing of Fe impurities in Pt. Spin-glass freezing was found for *Pd*-Fe with $T_f/x = 83\ \mu$K/at ppm Fe, but surprisingly was not observed for *Pt*-Fe to 76 μK even with 10–40 ppm Fe in Pt.[24]

5.4. Specific Heats

5.4.1. Specific Heat of the First Nuclear Stage

The specific heat of the first nuclear stage was measured in 2, 5, 6, and 40 mT and between 30 μK and 20 mK. For these measurements nothing was connected to the bottom of the first nuclear stage. In Fig. 16 we show the 2-, 6-, and 40-mT data and the calculated specific heats of the nuclear stage. The agreement is good (3%) for the 40-mT data, but there is an additional contribution at 2 and 6 mT for the higher temperatures. This additional contribution has a maximum of about 40 mJ/K at about 0.5 mK (see Fig. 17). Assuming its source is magnetic hyperfine interaction in Cu, we would need 7 mmole experiencing the rather large effective interaction of $B_{\text{int}} \simeq 1.4$ T. However, since the extra contribution does not depend on magnetic field (Figs. 16 and 17), it seems to result from a quadrupole

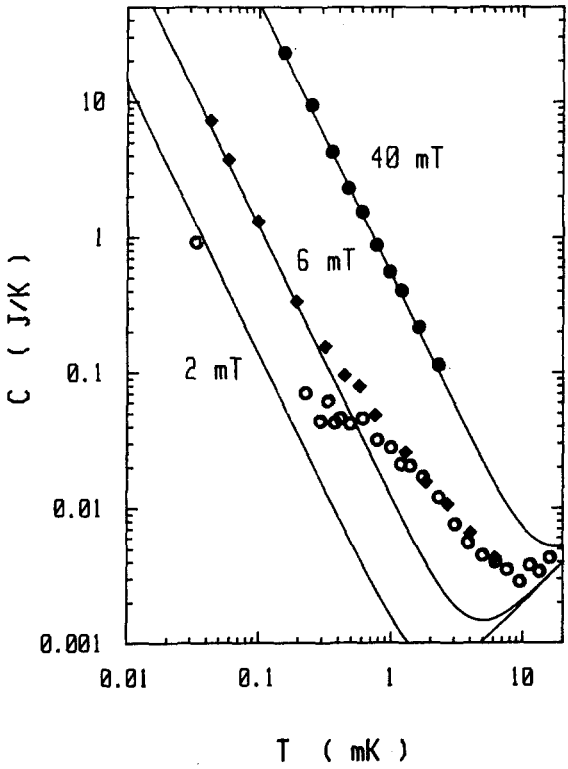

Fig. 16. Specific heat of the first nuclear stage in fields of (●) 40, (◆) 6, and (○) 2 mT as a function of temperature. (—) The nuclear plus electronic specific heat of the first nuclear stage in the given fields. The temperature scale is the measured electronic temperature. For the more appropriate nuclear temperature, the scale would have to be corrected by 1, 5, and 45% for the 40-, 6-, and 2-mT data, respectively, if the heat leak is 0.5 nW, for example.

hyperfine interaction. The electric field gradient necessary to explain our data is about 10^{18} V/cm^2 acting on 11 mmole with spin 3/2 and a quadrupole moment of 0.15 barn, the data for ^{63,65}Cu. This is a large but not unusual value for field gradients produced by impurities or defects in metal lattices; for example, electric field gradients at vacancies or vacancy complexes in Cu range from 3×10^{17} to 10×10^{17} V/cm.[25]

5.4.2. Specific Heat of the Second Nuclear Stage plus Platform and Thermal Link

The specific heat of the second nuclear stage (plus Cu platform and thermal link) was measured in two runs with the heat switch to the first

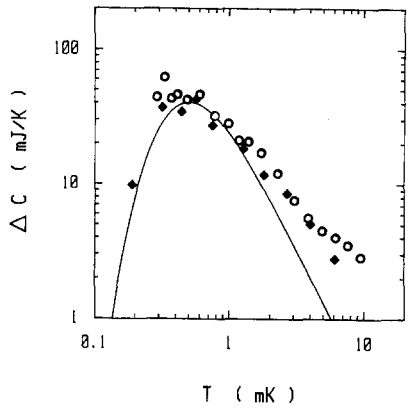

Fig. 17. Difference between the measured and calculated specific heat of the first nuclear stage (see Fig. 16) as a function of temperature. (—) The calculated nuclear quadrupole specific heat of 11 mmole Cu in a field gradient of about 10^{18} V/cm^2. The temperature scale is the measured electronic temperature. Correcting to nuclear temperatures has a negligible influence on (◆) the 6-mT data, but would shift (○) the 2-mT data somewhat to the lower left.

stage open (Fig. 18). At $6 < T_n < 22\ \mu$K with the Pb heat switch between the second stage (in 7 mT) and the platform the measured and calculated specific heat values agree quite well, as was also found for the first-stage specific heat at low temperatures (Fig. 16). At higher temperatures the specific heat was measured without heat switch between second stage and platform, hence there may be contributions from the platform plus addenda. As observed for the first stage, we find a substantial excess specific heat with a maximum of $\Delta C \simeq 12$ mJ/K at $T \simeq 0.6$ mK. If it would result from a magnetic hyperfine interaction in Cu, we would need about 2 mmole in an effective field of about 1.7 T, and for a quadrupole hyperfine interaction we need 3.5 mmole experiencing a field gradient of about 10^{18} V/cm^2.

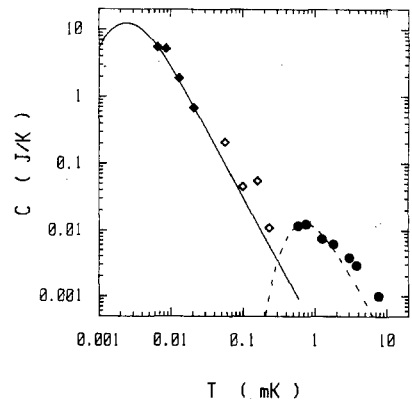

Fig. 18. Specific heat of the second nuclear stage (plus platform). The data have been taken with the following fields on the second nuclear stage: (◆) 7 mT, (◇) 14 mT, but divided by four to correct to 7 mT; (●) 6.8 mT. (—) The nuclear magnetic specific heat of 2 mole Cu in 7 mT. (- -) the nuclear quadrupole specific heat of 3.5 mmole Cu in a field gradient of about 10^{18} V/cm^2.

6. POSSIBLE ORIGINS OF THE EXCESS SPECIFIC HEAT AND OF THE INTERNAL HEAT LEAKS

6.1. Excess Specific Heat

Because the observed excess ΔC is rather similar for the two stages—in spite of their rather different masses—we have to search for a common origin. First, we exclude the possibility that the excess specific heat is an apparent effect due to anomalies from our Pt thermometers, or from overheating the Pt–W heaters and electrons of the Cu stage when we apply heat to measure the specific heat (we have changed the heating power without affecting the results).

As another common source one might suspect the Al_2O_3 rods used to support the stages and platform. For ^{27}Al, $I = 5/2$ and $Q = 0.149$ barn, but the measured quadrupole splitting in Al_2O_3 corresponds to $T < 0.1$ mK,[26] and therefore seems to be too small to explain our observation; the thermal time constant for the Al_2O_3 should also be very large.

Electronic contributions from magnetic impurities are rather unlikely origins because they should be either saturated (as for $3d$ impurities in Pt, which always sits at least in 6.8 mT) or they form Kondo states (as for $3d$ impurities in Cu). The amount of these impurities in our high-purity Cu or in thermometers and heaters is too small to consider them as the origin. In addition, the field independence seems to be a clear indication against a magnetic character of ΔC. This leaves nuclear quadrupole hyperfine interactions to explain our results.

We have about 21 g of BeCu with about 2 wt % Be on the first stage. It could be that Be distorts the Cu lattice enough so that its nearest Cu neighbors see an electric field gradient large enough to produce the observed ΔC (Be itself has a very small nuclear quadrupole moment). So the amount would be more than enough to explain our observation. In a search for the possible origin of the excess specific heat observed for the first nuclear stage, we therefore increased the amount of BeCu on this stage. The results were not conclusive, because we saw an increase of ΔC (three times) which was not proportional to the increase of BeCu (six times). In addition, there is no BeCu on the second stage and platform (second version), where we observe a ΔC as well.

There are other possible origins of the observed ΔC if it is due to a nuclear quadrupole interaction. One is Cu nuclei near grain boundaries and/or impurities, which may produce the necessary electric field gradient. Because the Cu of the first nuclear stage is purer and shows much larger crystallites than the Cu of the second nuclear stage and of the platform, it is not unreasonable that the ΔC's do not scale with the Cu mass. Again, the necessary amount, some millimoles, is quite possible.

We conclude that the most likely explanation for the observed ΔC is a nuclear quadrupole splitting in Cu with a field gradient resulting from impurities (possibly also Be in the screws used or oxide on the surface of the stage) and/or from lattice imperfections. The tail on the high-temperature side of Figs. 17 and 18 may result from a distribution of field gradients in our samples.

Anomalies in the specific heat of a Cu nuclear stage have also been seen in the low-millikelvin range by other groups, for example, in the refrigerators of refs. 3–6 and 27. For the Tokyo refrigerator, the ΔC showed the very large maximum value of 0.45 J/K at 0.5 mK.[5]

In ref. 6 a nuclear specific heat proportional to T^{-2} and corresponding to an effective internal field of 0.35 T was measured at $1 \leq T \leq 5$ mK for hammered Cu flakes. The excess ΔC was considerably reduced by annealing the flakes, and was related to nuclear quadrupole interactions in the highly deformed flakes or in CuO. The excess of ΔC of ref. 2 corresponded to an effective field of 0.03 T. Formerly, Anderson and co-workers[28] and Greywall[29] also saw excess contributions in the specific heat of Cu with $\Delta C \simeq 25\text{–}40/T^2$ nJ/mole K at $30 < T < 200$ mK, which were of unknown origin. If related to the total amount of Cu, the high-T tails of the excess specific heats observed by us correspond roughly to $\Delta C_1 \simeq 0.3/T^2$ nJ/mole K and $\Delta C_2 \simeq 10/T^2$ nJ/mole K for our first and second stages, respectively, so they are comparable to or smaller than the mentioned observations by others.

6.2. Possible Origins of the Internal Heat Leaks

The understanding and reduction of heat leaks is a major concern in the construction of a nuclear refrigerator. Heat leaks from external sources are of minor importance in our apparatus. The heat leak to the first nuclear stage cannot, for example, come from parts at mixing chamber temperature. This was confirmed by varying the mixing chamber temperature between 4.5 and 30 mK. The heat leak at $T < 1$ mK also cannot be explained by heat evolving from the above-discussed excess specific heats, because these would be emptied within a few days of supplying the observed heat leak.

In Fig. 19 we show the time dependence of the heat leaks determined from the drift rates of the first and second nuclear stages of our apparatus and compare it to the heat leak in the Jülich nuclear refrigerator and to heat evolving from ortho-para conversion of H_2. The figure demonstrates that the fit to ortho-para conversion is not poor enough to exclude ortho-para conversion of minute traces of H_2 in Cu as an essential contribution to the observed $\dot{Q}$. The amounts necessary to explain the data would be only about 1.3, 0.2, and 0.02 ppm H_2 if referred to the total amount of Cu in the Jülich second stage, our second stage plus platform, and our first

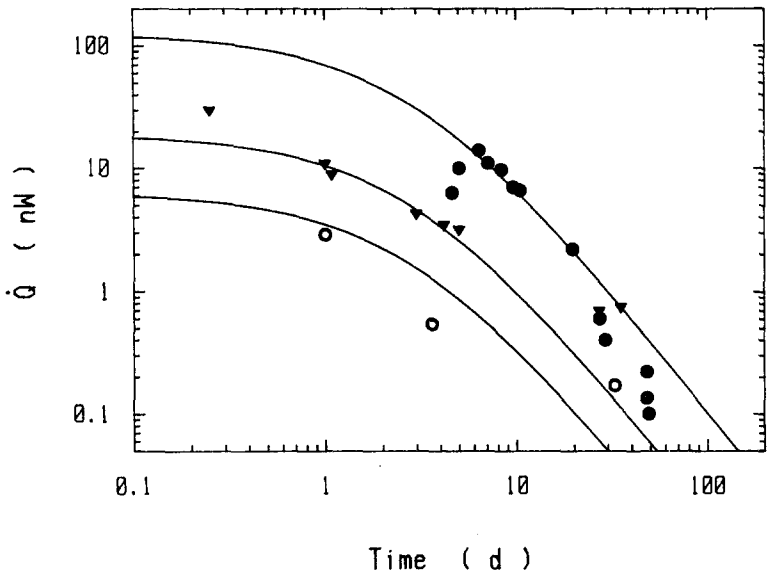

Fig. 19. Heat leak in (●) the Jülich nuclear refrigerator,[3,4] and in our (▼) first and (○) second nuclear stages, as a function of time after cooling to 4 K. (—) The heat leaks generated by ortho-para conversion of 40 μmole H_2, 6 μmole H_2, and 2 μmole H_2, respectively. These amounts correspond to 1.3, 0.02, and 0.2 ppm, respectively, if referred to the amounts of Cu.

stage, respectively. But there are other, likelier sources for the measured heat leaks.

The observed time dependence $\dot{Q} \propto t^{-3/4}$ at the first nuclear stage is similar to the one observed in several organic materials, e.g., Stycast 1266,[8] but the magnitude of $\dot{Q}$ would correspond to about 0.1 kg of Stycast 1266, an amount of organic material not present in our apparatus. This time dependence has been related to heat release from tunneling transitions of two-level states.[8] Such tunneling transitions could also result from molecules adsorbed on surfaces or from other "dirty" layers there; but the surface areas on the first stage (about 3 m^2) and on the second stage plus link and platform (about 0.1 m^2) are quite different, whereas the observed heat leaks are quite similar. In addition, the thickness of this heat-releasing surface area would have been unreasonably large to result in the observed energy release.[4]

The likeliest explanation of the observed time-dependent heat release is tunneling transitions of two-level states in the Cu stage (plus Ag and Pt) itself.[4,22] The total amount of heat released from our first nuclear stage (second nuclear stage plus platform and link) at low temperatures for $t \leq 50$

days is 10 (3) mJ. This corresponds to the relaxation of 0.4 (0.1) mmole of two-level tunneling states if they have an energy separation of 3 K, or about 1.5 (13) ppm in the metals of our first nuclear stage (second nuclear stage plus platform and link). The choice of $\Delta E/k_B = 3$ K is, of course, somewhat arbitrary, but we have to take into account that the heat leak was charged up again by warming the apparatus to 1 K (Fig. 11). The above numbers, 1.5 and 13 ppm, could be correlated with the purity of our Cu (and Ag), which is 6N for the first stage and 5N for the second stage. So we suggest that the density of states of heat-releasing two-level systems is associated with the impurities or defects (grain boundaries?) in our samples. The deviation of the observed time dependence from the standard tunneling model, $\dot{Q} \propto t^{-1}$, may result from a somewhat different energy distribution of tunneling states in imperfect crystalline metals as compared to glasses.

Increasing the amount of BeCu (used for screws on the heat switch) or switching to BeCu of other composition influenced the heat leak in a qualitative way and, for large amounts of BeCu, the adiabaticity of the demagnetization. This confirms that nonideal metals release heat at low temperatures.

Recently, it was also found that high-purity single-crystal silicon contains a density of two-level tunneling states only two orders of magnitude below the density of these states in vitreous silica, giving a total number of states of about 1 ppm or roughly equal to the concentration of impurities.[30]

It may seem somewhat surprising that the heat leak on the two nuclear stages is of the same order of magnitude even though their masses differ by about a factor of 30, but we have used higher quality Cu for the first stage than for the platform and second stage, and the first stage went through a more careful treatment.

Of course, we cannot rule out that the press contacts on the various joints of the first and second nuclear stages as well as on the Cu platform that result in deformations of the cubic Cu lattice may relax and give rise to time-dependent heat leaks (as well as to an excess nuclear quadrupole specific heat ΔC). The number and area of joints as well as the applied forces are quite comparable on the two stages. Low-temperature heat leaks from strain relaxation of press contacts have been observed earlier.[31] An interpretation of time-dependent, low-temperature heat leaks in Cu in terms of athermic relaxation phenomena has been given in ref. 32.

Even though the absolute values of the heat leak look somewhat high, they are rather small, of order 3 (10) pW/mole on the first (second) stage after 4 weeks below 4 K. Our results demonstrate that we are approaching a temperature and heat leak range where the performance of nuclear refrigerators may eventually be limited by natural radioactivity in the materials and by ionization from cosmic rays.[4] Assuming a mean flux of

cosmic rays of 2 cm^{-2} min^{-1} and an ionization energy of 2 MeV/g cm^{-2}, we find for our first nuclear stage $\dot{Q}_{cosmic} \approx 0.2$ nW or about 1 pW/mole.

7. CONCLUSIONS

We have constructed and operated a nuclear refrigerator which can refrigerate with one Cu stage (104 moles in 8 T) experiments in the field-free region of the apparatus to 15 μK, 3 weeks after cooldown, and to 20 μK already 1 week after cooldown. The refrigerator can keep experiments at 15 μK for at least 2 days, and can stay below 20 μK for more than 1 week. The demagnetization behaves adiabatically from 10 mK to at least 100 μK, also confirming our temperature calibration. Adding a second Cu stage (2 moles in 9 T) reduces the temperature to at most 12 μK (possibly to as low as 10 μK). The minimum temperatures seem to be mainly limited by a temperature gradient along the first nuclear stage resulting from an internal heat leak of order 1 nW, 3 weeks after cooldown, and by a heat reservoir residing in the parts between the first and second nuclear stages. Temperature gradients in the Pt NMR thermometers seem to be less likely as the limit for the minimum measured temperatures. We have also discussed the possibility of a nuclear magnetic ordering in Pt or a spin-glass freezing of $3d$ moments in Pt as a limit for the temperature indicated by our Pt thermometers.

In spite of the fact that we have strongly restricted the number and amount of materials in the refrigerator, besides the refrigerant Cu, we see annoying internal heat leaks $\dot{Q}$ and excess contributions ΔC to the specific heat. Nonetheless, for our first nuclear stage the heat leak per mole is substantially below the values observed in former nuclear refrigerators. We have discussed various possible origins for the heat leaks and for the excess specific heat, with the likeliest sources being nuclear quadrupole hyperfine interactions in Cu for ΔC and energy reservoirs resembling the behavior of tunneling transitions in noncrystalline materials in Cu and other metals for $\dot{Q}$; both may be caused by impurities and/or lattice imperfections in the metals. Additional contributions to $\dot{Q}$ may result from lattice strain relaxation and orth–para conversion of H_2 in Cu.

Because of the heat reservoir on the parts between first and second nuclear stages, we are planning a further improvement of the apparatus by reducing the mass of the parts between the stages, and by replacing the Cu there by Ag. The link between the two stages will be essentially a Ag rod interruped by Al for the thermal switch.

We have shown that one can design Pt NMR thermometers with very fast relaxation times in the microkelvin temperature range ($\tau \approx 9$ min at 15 μK). For the future it seems to be of importance to investigate the details

of Pt NMR thermometry in the low-microkelvin temperature range to exclude or investigate possible ordering transitions of Pt at these temperatures and in fields of a few mT. This question is particularly important for Pt of moderate purity, for which we have observed a very fast spin-lattice relaxation (4 sec at 1 mK and in 7 mT).

ACKNOWLEDGMENTS

We gratefully acknowledge the help and advice of W. Müller on various electronic problems, the help of Dr. J. M. Welter in melting and annealing the first nuclear stage, the expert work of our mechanical and electronic workshops, as well as contributions in the early stages of our work by Dr. C. Buchal, W. Bergs, J. Hanssen, and Dr. M. Jutzler.

REFERENCES

1. N. Kurti, F. N. Robinson, F. E. Simon, and D. A. Spohr, *Nature* **178**, 450 (1956).
2. R. G. Gylling, *Acta Polytech. Scand.* **Ph81** (1971); A. I. Ahonen, P. M. Berglund, M. T. Haikala, M. Krusius, O. V. Lounasmaa, and M. A. Paalanen, *Cryogenics* **16**, 521 (1976); M. C. Veuro, *Acta Polytech. Scand.* **Ph122** (1978).
3. R. M. Mueller, C. Buchal, H. R. Folle, M. Kubota, and F. Pobell, *Cryogenics* **20**, 395 (1980).
4. F. Pobell, *Physica B+C* **109/110**, 1485 (1982).
5. H. Ishimoto, N. Nishida, T. Furabayashi, M. Sinohara, Y. Takano, Y. I. Miura, and K. Ono, *J. Low Temp. Phys.* **55**, 17 (1984); and private communications.
6. D. I. Bradley, A. M. Guénault, V. Keith, C. J. Kennedy, I. E. Miller, S. G. Mussett, G. R. Pickett, and W. R. Pratt, Jr., *J. Low Temp. Phys.* **57**, 359 (1984).
7. G. Frossati, H. Godfrin, B. Hebral, G. Schuhmacher, and D. Thoulouze, in *Physics at Ultralow Temperatures*, T. Sugawara, ed. (Physical Society of Japan, Tokyo, 1978, p. 205; G. Frossati, *J. Phys. (Paris)* **39**, C6-1578 (1978).
8. M. Schwark, F. Pobell, W. P. Halperin, C. Buchal, J. Hanssen, M. Kubota, and R. M. Mueller, *J. Low Temp. Phys.* **53**, 685 (1983); M. Schwark, F. Pobell, M. Kubota, and R. M. Mueller, *J. Low Temp. Phys.* **58**, 171 (1985).
9. A. C. Tims, R. L. Davidson, and R. W. Timme, *Rev. Sci. Instr.* **46**, 554 (1975).
10. U. Angerer and G. Eska, *Cryogenics* **53**, 515 (1984).
11. K. Gloos, P. Smeibidl, and F. Pobell, to be published.
12. J. P. Pekola, J. T. Simola, and K. K. Numila, in *Proceedings of the 10th International Cryogenic Engineering Conference*, H. Collan, P. Berglund, and M. Krusius, eds. (Butterworths, London, 1984), p. 259.
13. R. M. Mueller, C. Buchal, T. Oversluizen, and F. Pobell, *Rev. Sci. Instr.* **49**, 515 (1978).
14. M. Jutzler, B. Schröder, K. Gloos, and F. Pobell, *Z. Phys.* B **64**, 115 (1986).
15. C. Buchal, J. Hanssen, R. M. Mueller, and F. Pobell, *Rev. Sci. Instr.* **49**, 515 (1978).
16. G. Eska, *J. Low Temp. Phys.* **73**, 207 (1988).
17. O. Avenel, P. Berglund, and E. Varoquaux, unpublished, quoted in ref. 18.
18. D. O. Edwards, J. D. Feder, W. J. Gully, G. G. Ihas, J. Landau, and K. A. Muething, in *Physics at Ultralow Temperatures*, T. Sugawara, ed. (Physical Society of Japan, 1978), p. 280.
19. R. Ling, E. R. Dobbs, and J. Saunders, *Phys. Rev.* B **33**, 629 (1986).
20. W. A. Roshen and W. F. Saam, *Phys. Rev.* B **22**, 5495 (1980); and unpublished results.
21. J. Kästner, E. F. Wassermann, K. Matho, and J. L. Tholence, *J. Phys.* F **8**, 103 (1978).
22. M. T. Huiku, T. A. Jyrkkiö, J. M. Kyynäräinen, M. T. Loponen, O. V. Lounasmaa, and A. S. Oja, *J. Low Temp. Phys.* **62**, 433 (1986).

23. P. Kumar, J. Kurkijärvi, and A. S. Oja, *Phys. Rev.* B **33**, 444 (1986).
24. R. P. Peters, Ch. Buchal, M. Kubota, R. M. Mueller, and F. Pobell, *Phys. Rev. Lett.* **53**, 1108 (1984).
25. O. Echt, E. Recknagel, A. Weidinger, and Th. Wichert, *Z. Phys.* B **32**, 59 (1978).
26. A. Abragam, *Principles of Nuclear Magnetism* (Clarendon Press, Oxford, 1983), p. 235.
27. O. Avenel and E. Varoquaux, private communication.
28. G. J. Sellers and A. C. Andersson, *Rev. Sci. Instr.* **45**, 1256 (1974); E. J. Cotts and A. C. Andersson, *J. Low Temp. Phys.* **43**, 437 (1981).
29. D. S. Greywall, *Phys. Rev.* B **18**, 2127 (1978).
30. R. N. Kleiman, G. Agnolet, and D. J. Bishop, *Phys. Rev. Lett.* **59**, 2079 (1987).
31. D. S. Osheroff and W. Sprenger, private communication.
32. B. S. Neganov and V. N. Trofimov, *JETP Lett.* **28**, 328 (1978); V. N. Trofimov, *J. Low Temp. Phys.* **54**, 555 (1984).